Electronic Supplementary Information

Synergistic catalysis in Ni/ZrO_x for hydrogen production from hydrolysis of ammonia borane

Yong Li,[a,b] Shijie Zhou,[a] Xingyue Yang,[a] Enze Xu,[a] Zhen Ren,[a] Lei Wang,[a] and Yusen Yang*[a]

[a] State Key Laboratory of Chemical Resource Engineering, Beijing Advanced Innovation Center for Soft Matter Science and Engineering, Beijing University of Chemical Technology, Beijing 100029, P. R. China

[b] Grease Branch, Sinopec Lubricant CO., LTD, Tianjin 300480, P. R. China

Author Information

***** Corresponding author. Tel: +86-10-64412131; Fax: +86-10-64425385.

E-mail address: yangyusen@mail.buct.edu.cn (Y. Yang).

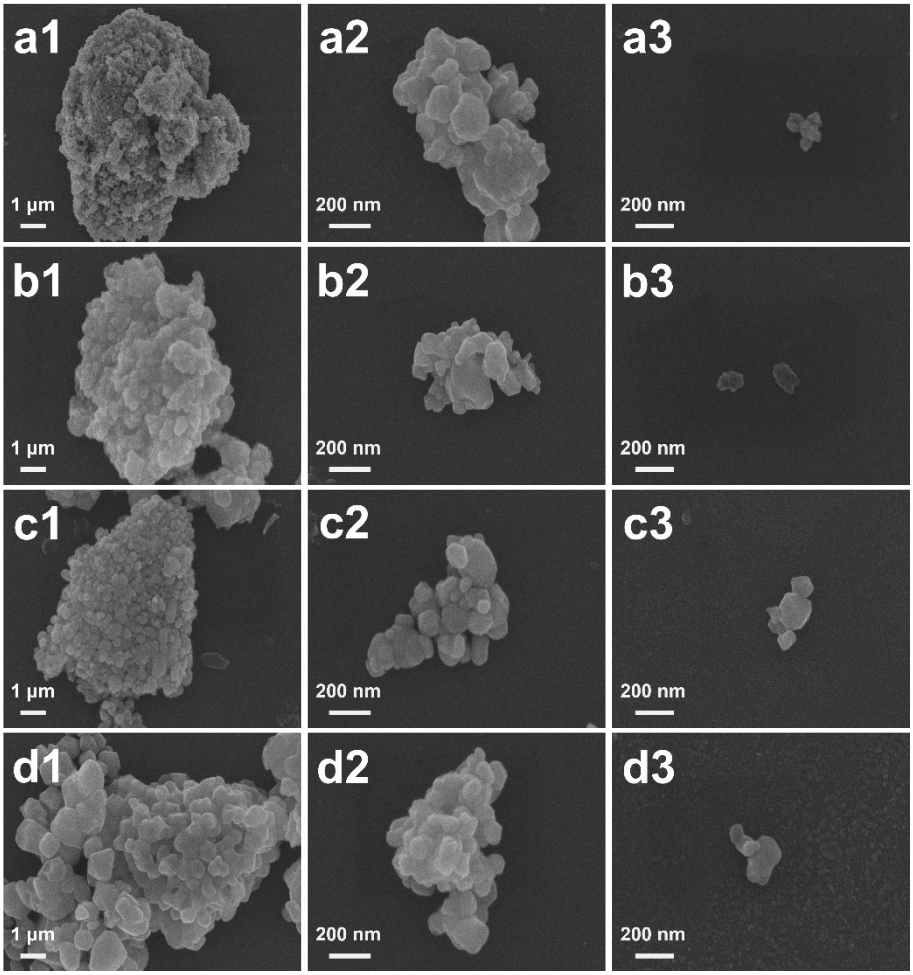

Fig. S1. SEM images of the as-synthesized ZrO_x-T samples: (a1−a3) ZrO_x-300, (b1−b3) ZrO_x-400, (c1−c3) ZrO_x-500 and (d1−d3) ZrO_x-600, respectively.

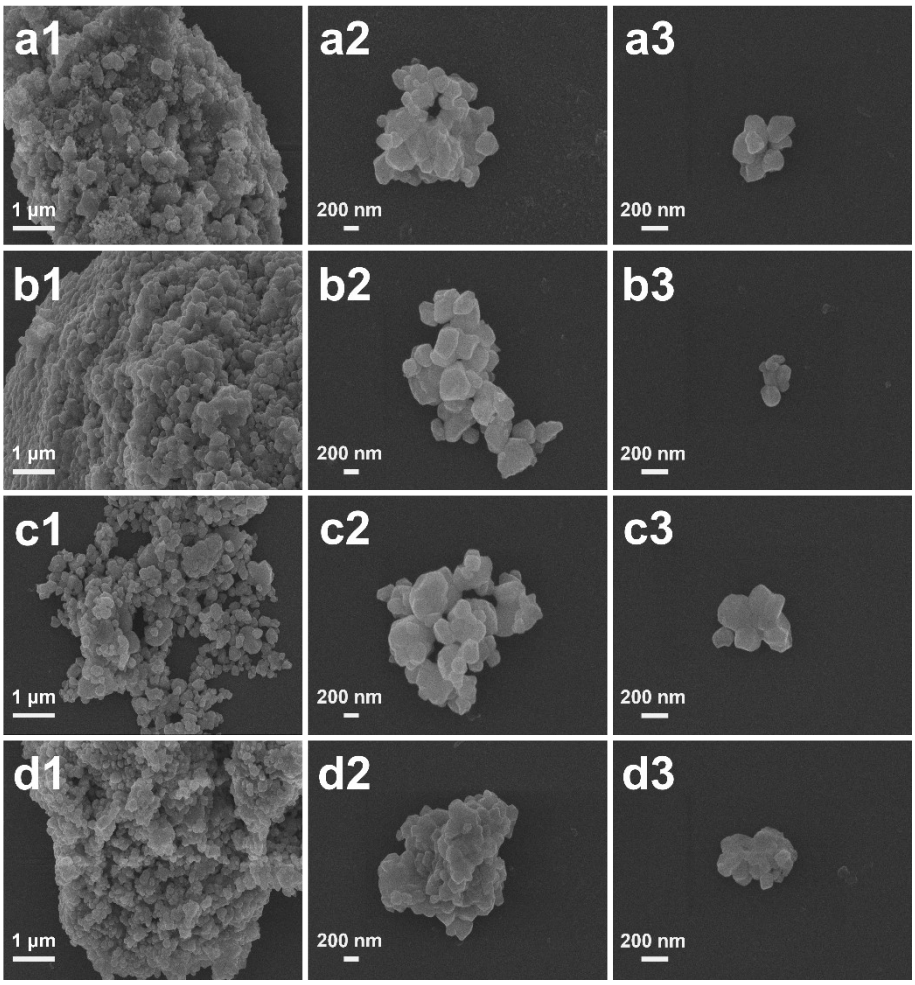

Fig. S2. SEM images of the as-synthesized Ni/ZrO_x-T samples: (a1−a3) Ni/ZrO_x-300, (b1−b3) Ni/ZrO_x-400, (c1−c3) Ni/ZrO_x-500 and (d1−d3) Ni/ZrO_x-600, respectively.

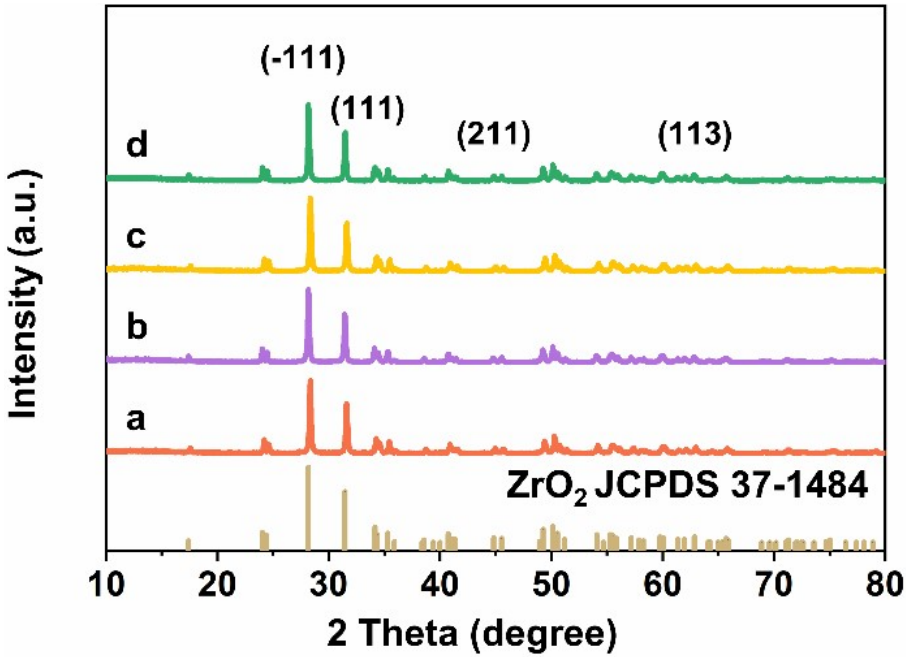

Fig. S3. XRD patterns of the as-synthesized ZrO_x-T samples: (a) ZrO_x-300, (b) ZrO_x-400, (c) ZrO_x-500 and (d) ZrO_x-600. XRD standard card for ZrO_2 is shown in the lower part of panel: ZrO_2-PDF#37-1484.

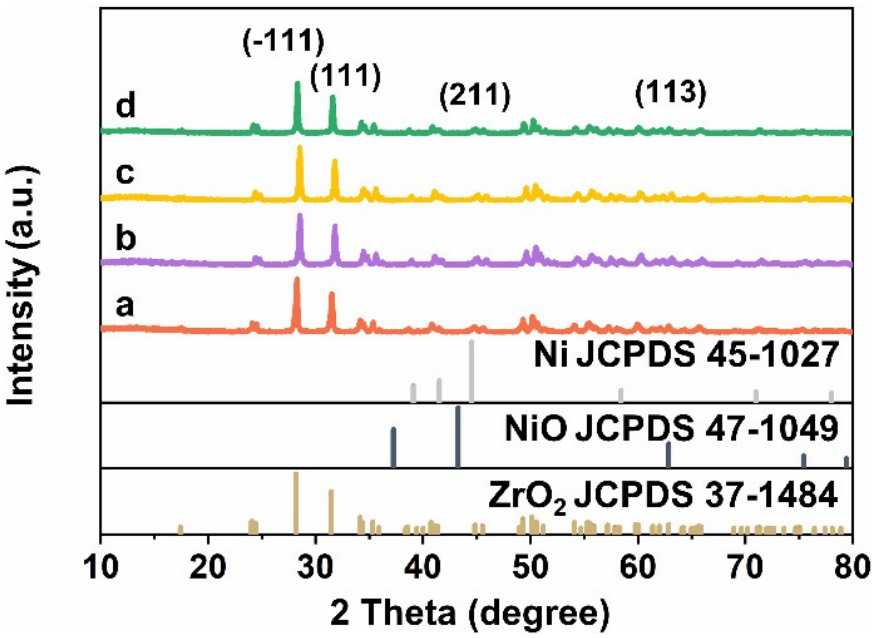

Fig. S4. XRD patterns of the as-synthesized Ni/ZrO_x-T samples: (a) Ni/ZrO_x-300, (b) Ni/ZrO_x-400, (c) Ni/ZrO_x-500 and (d) Ni/ZrO_x-600. XRD standard cards for Ni, NiO and ZrO_2 are shown in the lower part of the panel: Ni-PDF#45-1027, NiO-PDF#47-1049 and ZrO_2-PDF#37-1484.

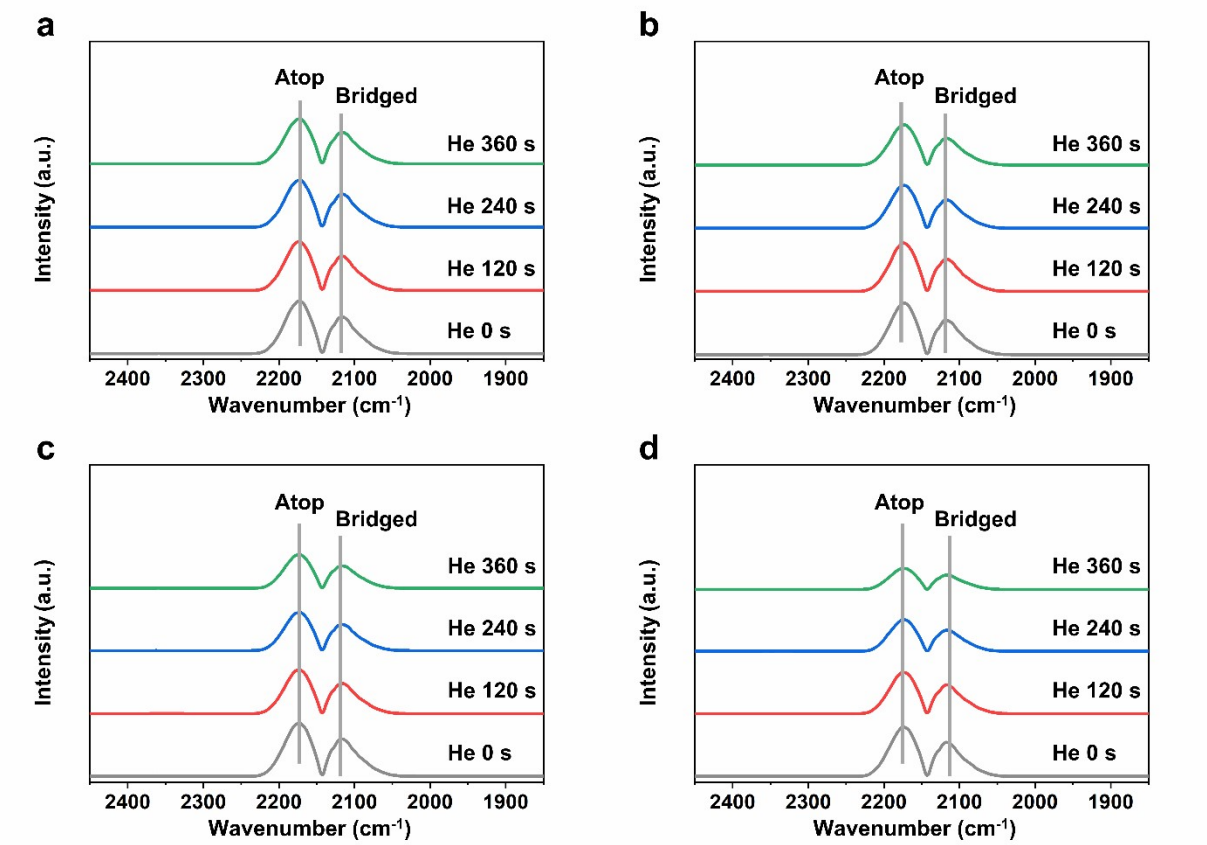

Fig. S5. *In situ* FT-IR spectra of CO chemisorption on (a) Ni/ZrO_x-300, (b) Ni/ZrO_x-400, (c) Ni/ZrO_x-500 and (d) Ni/ZrO_x-600 by flowing He as a purge gas after 0, 120, 240 and 360 s, respectively.

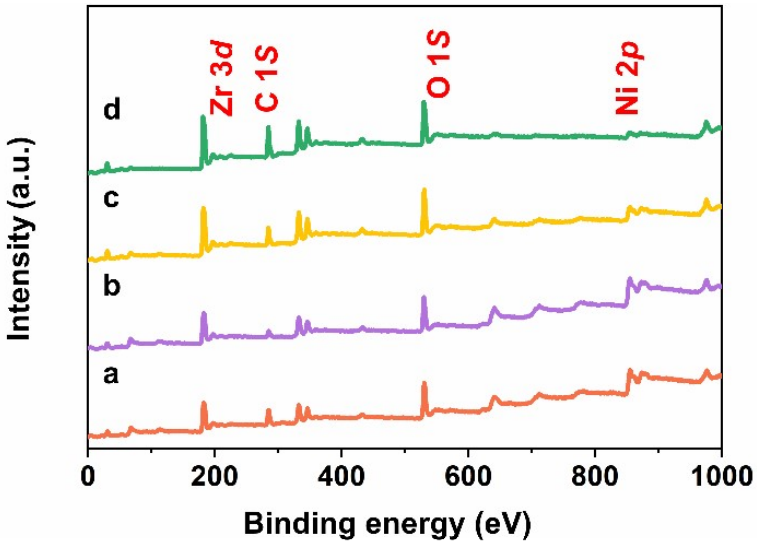

Fig. S6. XPS spectra of (a) Ni/ZrO_x-300, (b) Ni/ZrO_x-400, (c) Ni/ZrO_x-500 and (d) Ni/ZrO_x-600, respectively.

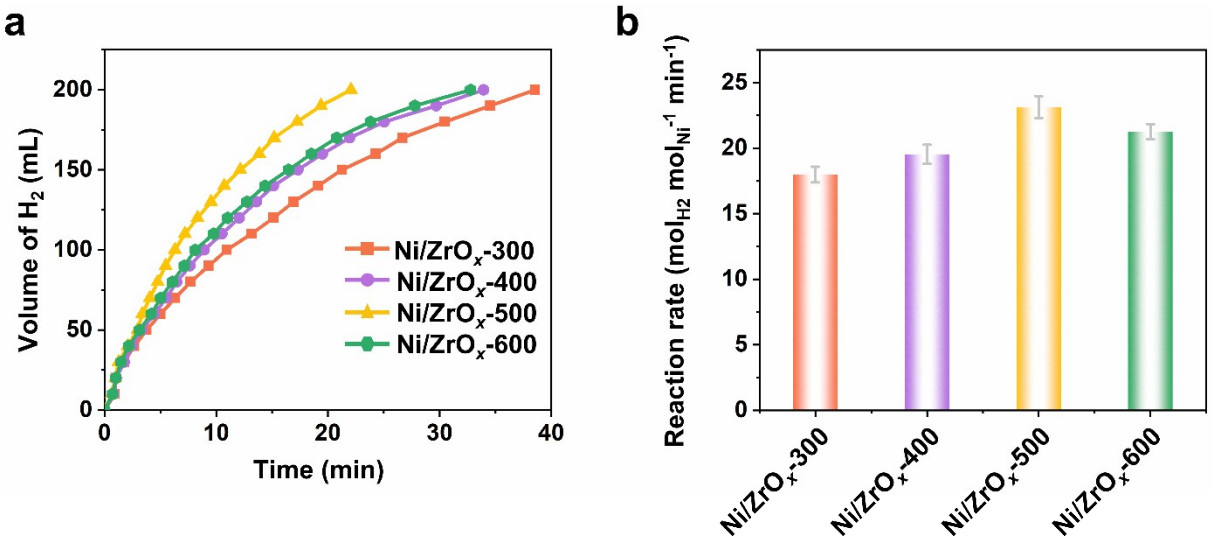

Fig. S7. (a) Plot of volume of H_2 *vs*. reaction time without NaOH for Ni/ZrO_x-T samples, and (b) the corresponding reaction rate values. Reaction conditions: (a) AB: 3.0 mmol, NaOH: 0 mmol, H_2O: 10 mL, catalyst: 40.0 mg, temperature: 25 °C.

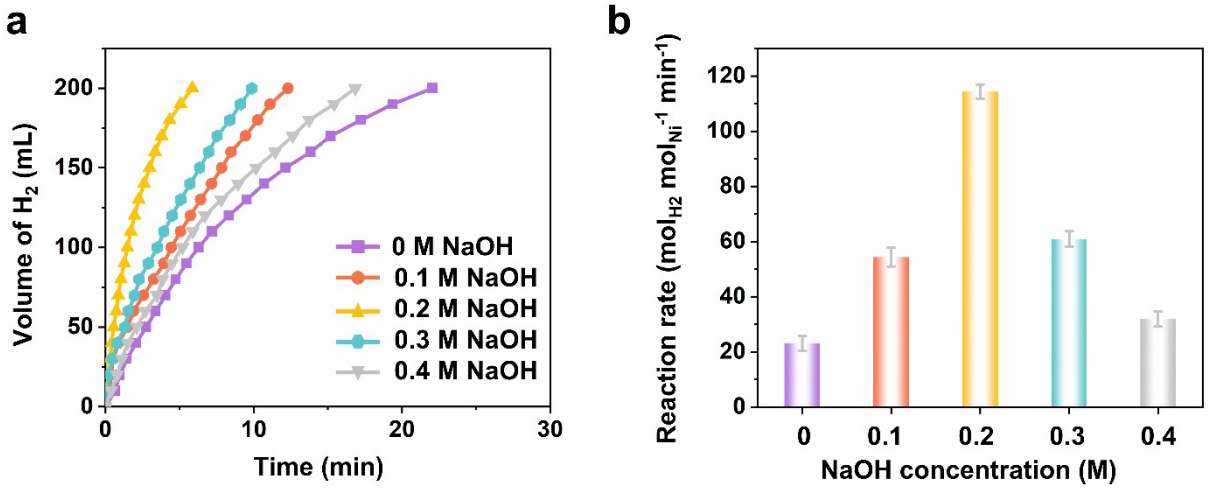

Fig. S8. (a) Plot of volume of H_2 *vs*. reaction time for Ni/ZrO_x-500 with different NaOH concentrations (0−4 M). (b) Effect of NaOH concentration on the reaction rate for Ni/ZrO_x-500. Reaction conditions: (a) AB: 3.0 mmol, NaOH: 0−40 mmol, H_2O: 10 mL, catalyst: 40.0 mg, temperature: 25 °C.

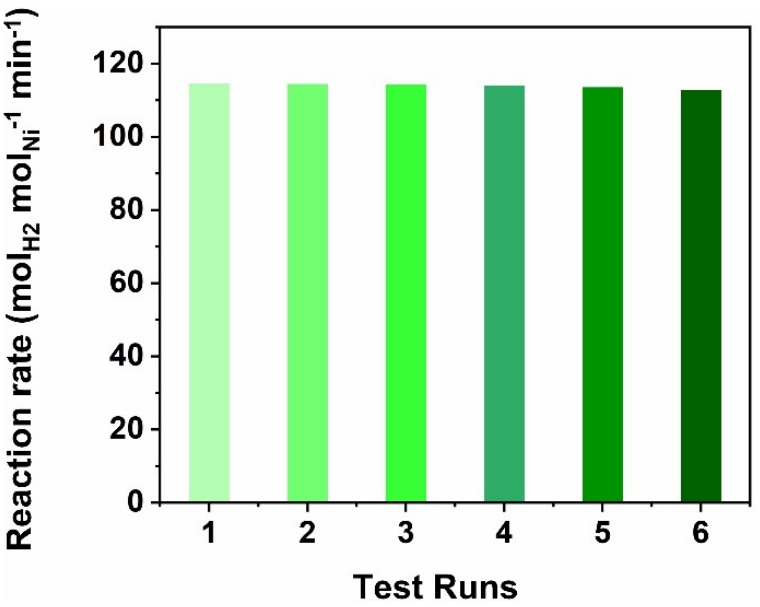

Fig. S9. Reaction rate of AB hydrolysis *vs*. recycling times over Ni/ZrO_x-500.

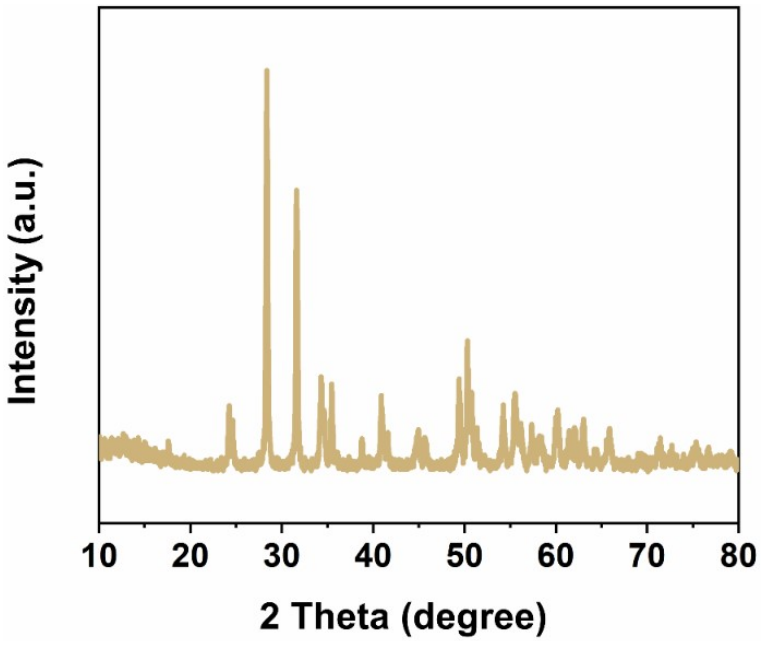

Fig. S10. XRD pattern of the used Ni/ZrO_x-500 sample.

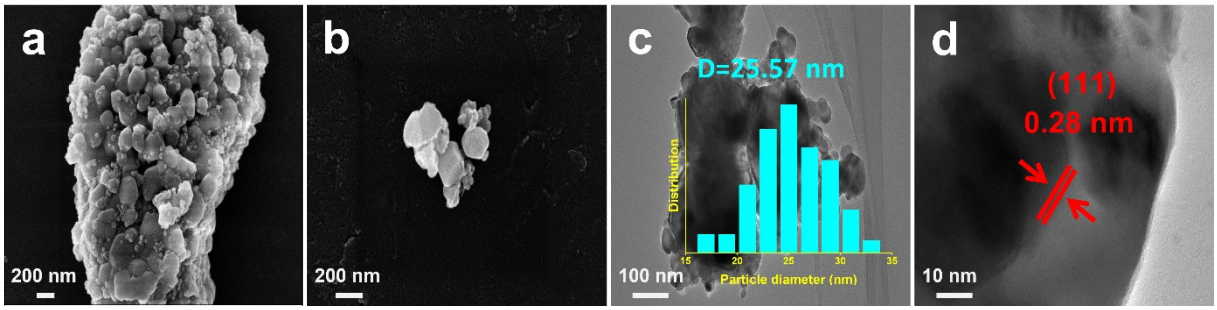

Fig. S11. (a–b) SEM images and (c–d) HR-TEM images of the used Ni/ZrO_x-500 sample with corresponding HR-TEM lattice fringe images.

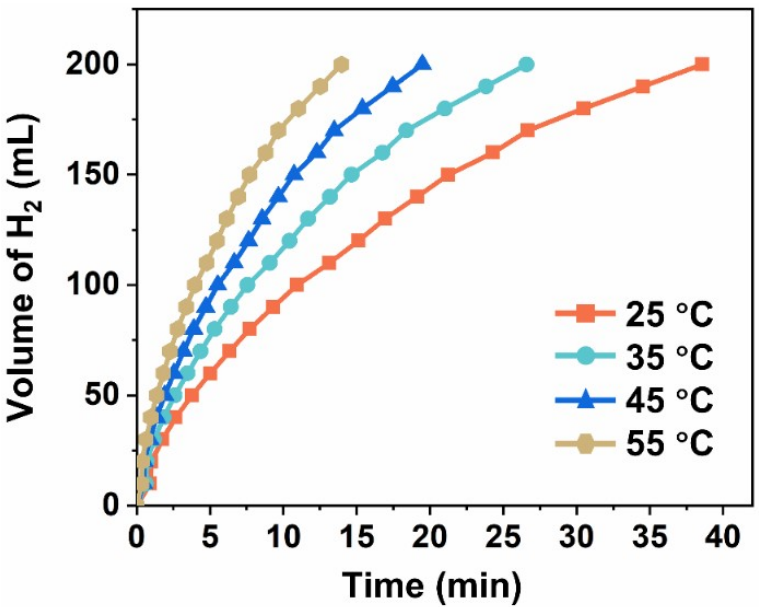

Fig. S12. Plot of volume of H_2 *vs*. reaction time for Ni/ZrO_x-300 under different reaction temperature (25−55 °C).

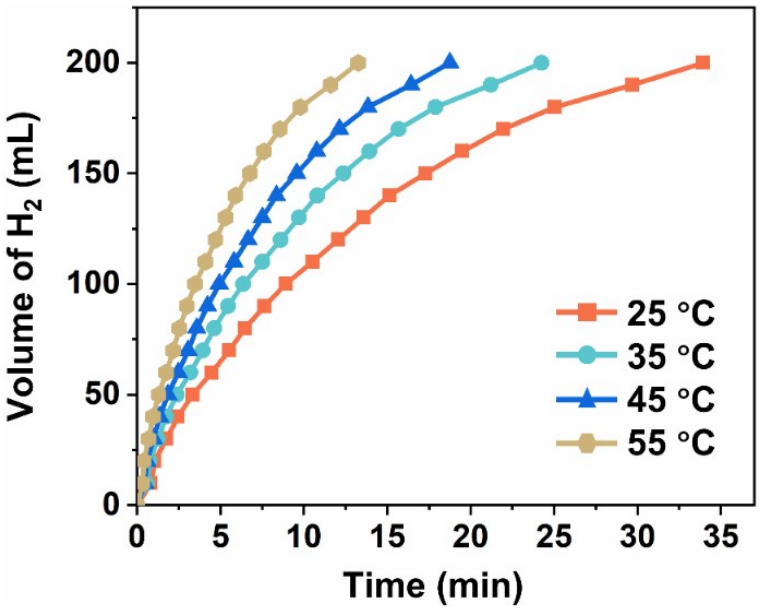

Fig. S13. Plot of volume of H_2 *vs*. reaction time for Ni/ZrO_x-400 under different reaction temperature (25−55 °C).

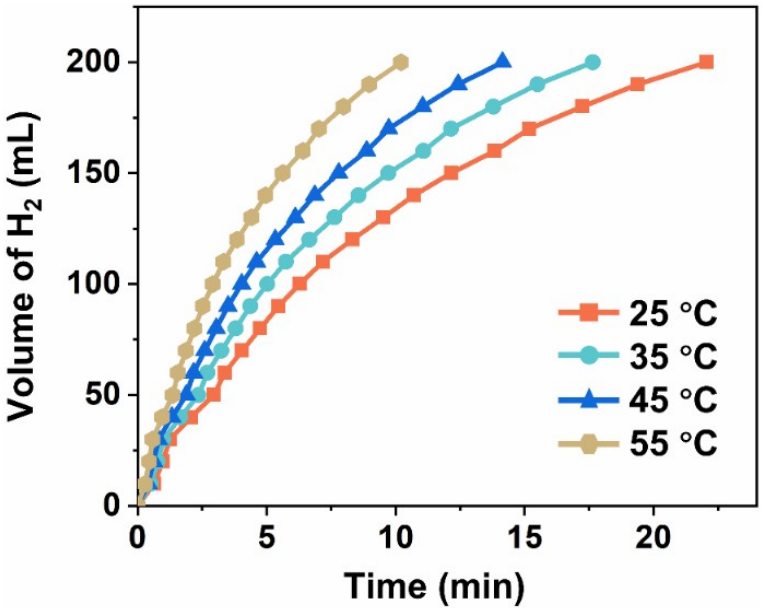

Fig. S14. Plot of volume of H_2 *vs*. reaction time for Ni/ZrO_x-500 under different reaction temperature (25−55 °C).

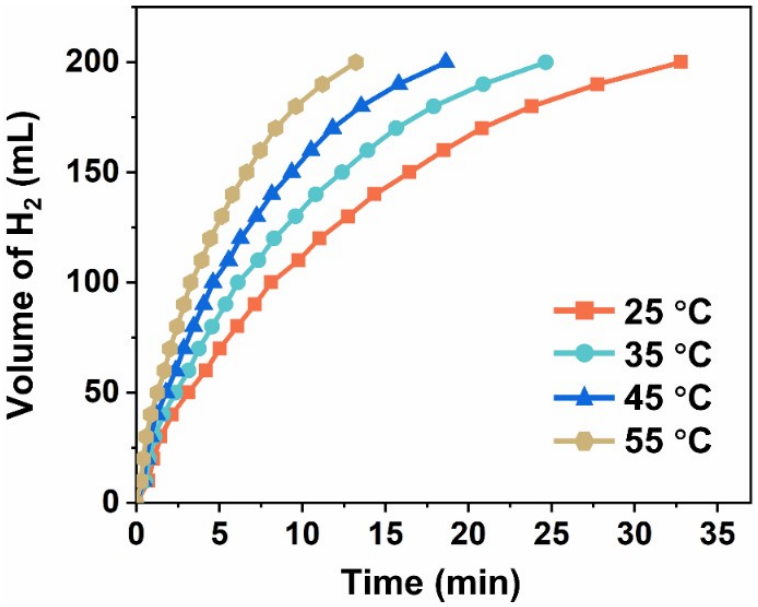

Fig. S15. Plot of volume of H_2 *vs*. reaction time for Ni/ZrO_x-600 under different reaction temperature (25−55 °C).

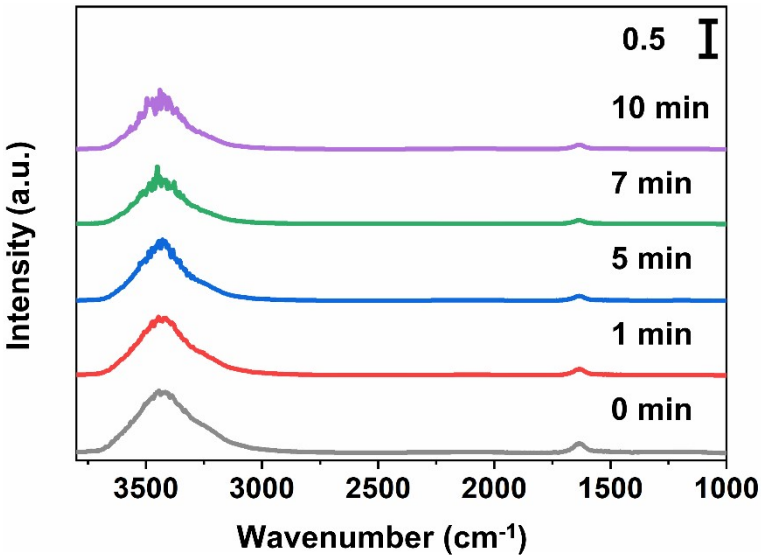

Fig. S16. *In situ* FT-IR spectra of AB hydrolysis reaction on ZrO_x-500 sample recorded in 3800−1000 cm^{-1} by flowing AB solution as a reaction gas and He as a purge gas after 0, 1, 5, 7 and 10 min, respectively.

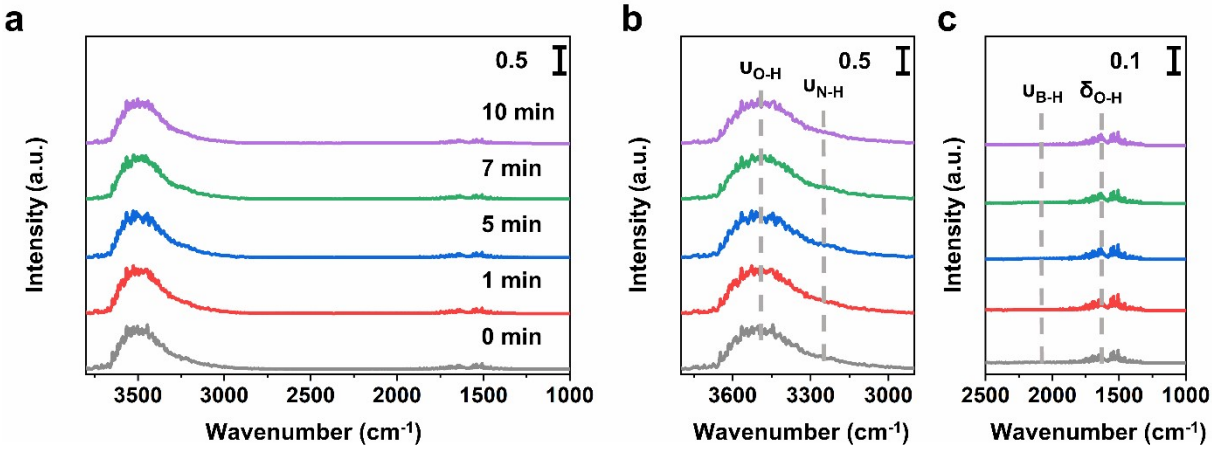

Fig. S17. *In situ* FT-IR spectra of AB hydrolysis reaction on KBr sample recorded in (a) 3800−1000 cm^{-1}, (b) 3800−2900 cm^{-1} and (c) 2500−1000 cm^{-1} by flowing AB solution as a reaction gas and He as a purge gas after 0, 1, 5, 7 and 10 min, respectively.

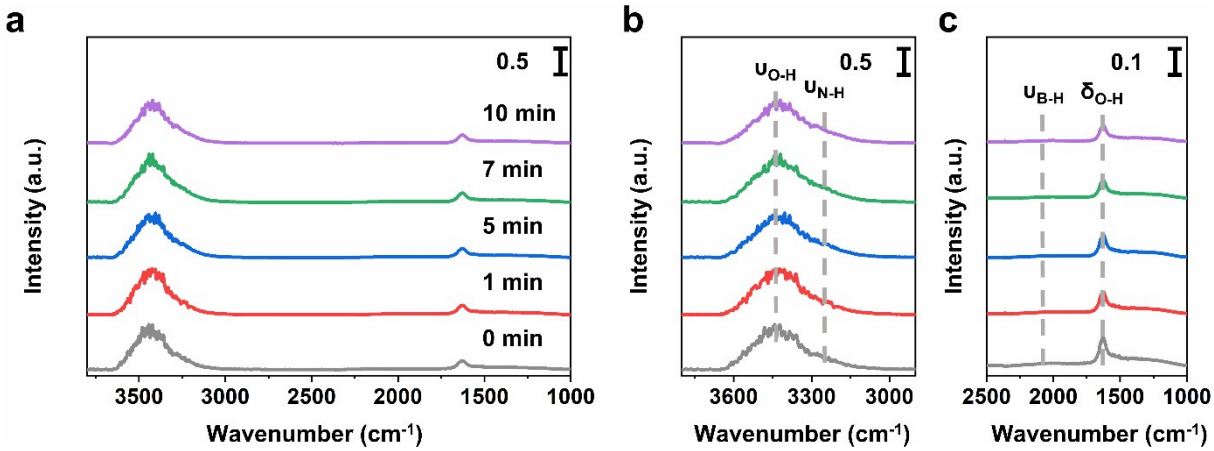

Fig. S18. *In situ* FT-IR spectra of AB hydrolysis reaction on Ni/ZrO_x-300 sample recorded in (a) 3800−1000 cm^{-1}, (b) 3800−2900 cm^{-1} and (c) 2500−1000 cm^{-1} by flowing AB solution as a reaction gas and He as a purge gas after 0, 1, 5, 7 and 10 min, respectively.

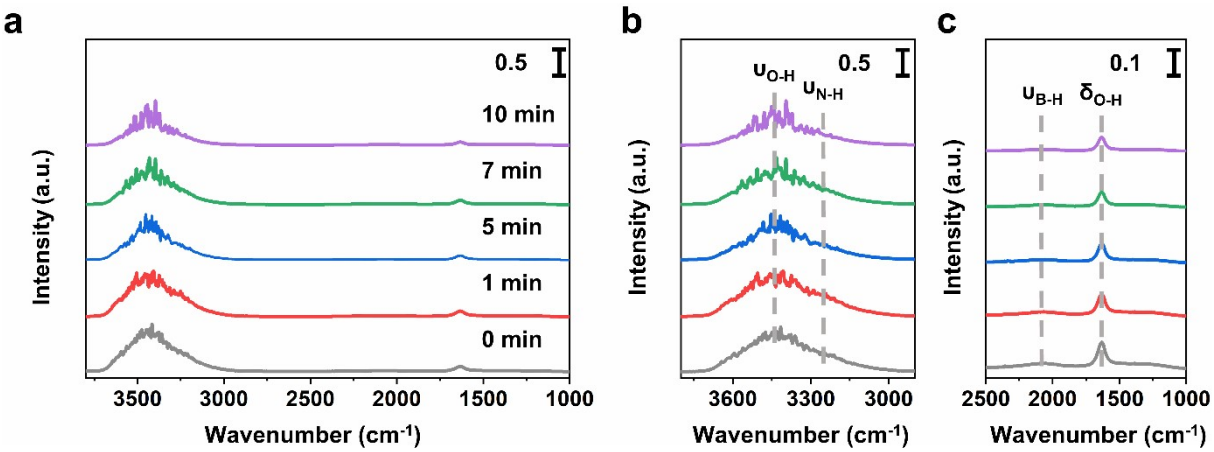

Fig. S19. *In situ* FT-IR spectra of AB hydrolysis reaction on Ni/ZrO_x-400 sample recorded in (a) 3800−1000 cm^{-1}, (b) 3800−2900 cm^{-1} and (c) 2500−1000 cm^{-1} by flowing AB solution as a reaction gas and He as a purge gas after 0, 1, 5, 7 and 10 min, respectively.

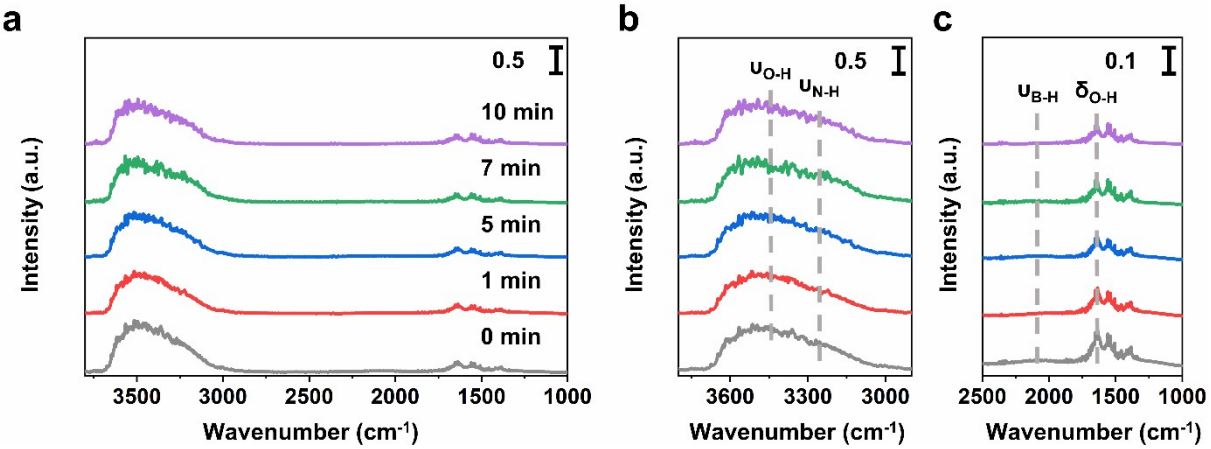

Fig. S20. *In situ* FT-IR spectra of AB hydrolysis reaction on Ni/ZrO_x-600 sample recorded in (a) 3800−1000 cm^{-1}, (b) 3800−2900 cm^{-1} and (c) 2500−1000 cm^{-1} by flowing AB solution as a reaction gas and He as a purge gas after 0, 1, 5, 7 and 10 min, respectively.

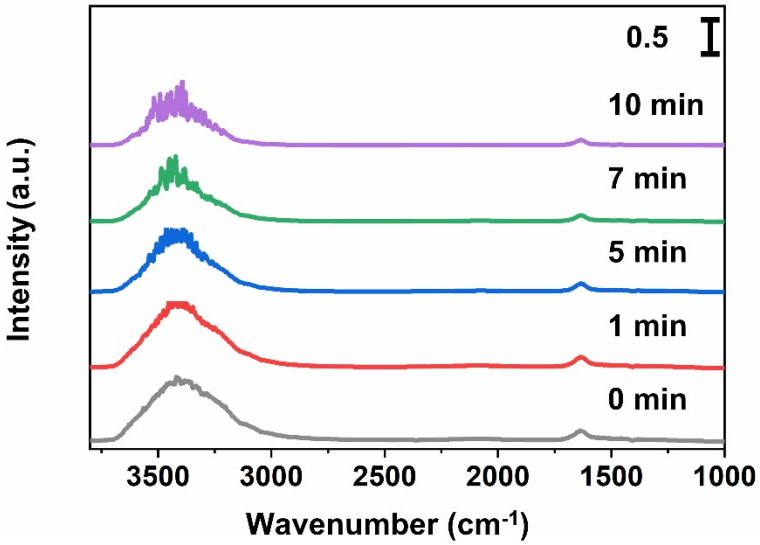

Fig. S21. *In situ* FT-IR spectra of AB hydrolysis reaction on Ni/ZrO_x-500 sample recorded in 3800−1000 cm^{-1} by flowing AB solution as a reaction gas and He as a purge gas after 0, 1, 5, 7 and 10 min, respectively.

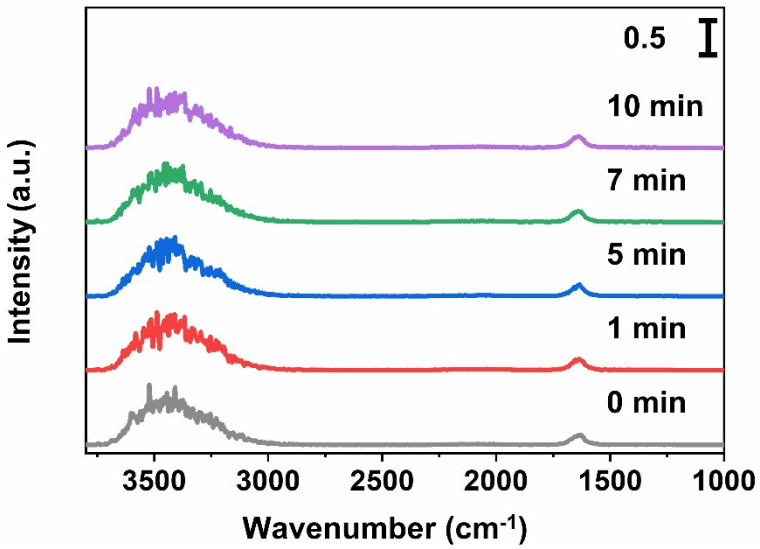

Fig. S22. *In situ* FT-IR spectra of ZrO_x-500 sample recorded in 3800−1000 cm^{-1} by flowing pure H_2O with He as a purge gas after 0, 1, 5, 7 and 10 min, respectively.

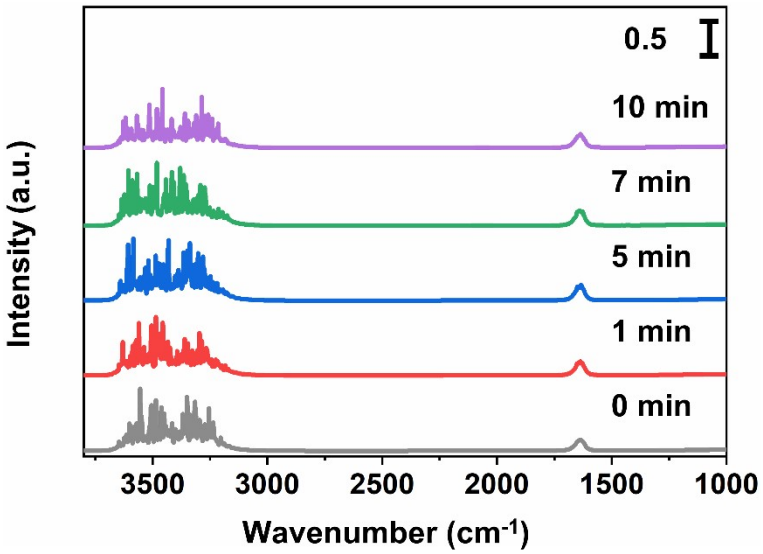

Fig. S23. *In situ* FT-IR spectra of Ni/ZrO_x-500 sample recorded in 3800−1000 cm^{-1} by flowing pure H_2O with He as a purge gas after 0, 1, 5, 7 and 10 min, respectively.

Table S1. Physicochemical properties of Ni/ZrO_x-T samples

Entry	Catalyst	Ni content (*wt.*%)[a]	Ni content in the filtration liquid (*wt.*%)[a]	Zr content in the filtration liquid (*wt.*%)[a]	Mean particle size of Ni (nm)[b]	Theoretical dispersion degree of Ni[c]
1	Ni/ZrO_x-300	4.579	/	/	22.27	2.28%
2	Ni/ZrO_x-400	4.667	/	/	22.35	2.27%
3	Ni/ZrO_x-500	4.453	/	/	23.20	2.19%
4	Ni/ZrO_x-600	4.516	/	/	28.33	1.79%

[a] Content of Ni and Zr species was determined by inductively coupled plasma-atomic emission spectroscopy (ICP-AES).

[b] Mean particle size of Ni was determined by HR-TEM analysis over 100 particles for each sample.

[c] Theoretical dispersion of Ni was calculated based on the result of HR-TEM.

Table S2. Compositional properties of Ni/ZrO_x-T samples

Entry	Catalyst	$Ni^{2+}/(Ni^0+Ni^{2+})$ ratio[a]	$Zr^{3+}/(Zr^{3+}+Zr^{4+})$ ratio[b]	$O_v/(O_v+O_l+O_s)$ ratio[c]
1	Ni/ZrO_x-300	42.10%	32.96%	19.88%
2	Ni/ZrO_x-400	47.28%	60.42%	26.91%
3	Ni/ZrO_x-500	58.13%	84.64%	38.01%
4	Ni/ZrO_x-600	50.41%	75.55%	34.89%

[a] $Ni^{2+}/(Ni^0+Ni^{2+})$ ratio was calculated from Ni 2*p* XPS spectra.

[b] $Zr^{3+}/(Zr^{3+}+Zr^{4+})$ ratio was calculated from Zr 3*d* XPS spectra.

[c] $O_v/(O_v+O_l+O_s)$ ratio was calculated from O 1*s* XPS spectra.

Table S3. Reaction rates for AB hydrolysis over Ni/ZrO_x-T and ZrO_x-T catalysts

Entry	Sample[a]	Reaction condition	Reaction rate (mol_{H2} mol_{Ni}^{-1} min^{-1})
1	Ni/ZrO_x-300	0 M NaOH	17.99±0.60
2	Ni/ZrO_x-400	0 M NaOH	19.53±0.73
3	Ni/ZrO_x-500	0 M NaOH	23.13±0.83
4	Ni/ZrO_x-600	0 M NaOH	21.26±0.58
5	Ni/ZrO_x-500	0.1 M NaOH	54.38±3.41
6	Ni/ZrO_x-500	0.2 M NaOH	114.41±2.58
7	Ni/ZrO_x-500	0.3 M NaOH	60.93±2.77
8	Ni/ZrO_x-500	0.4 M NaOH	31.90±2.70
9	/	0.2 M NaOH	0±0
10	Ni/ZrO_x-300	0.2 M NaOH	38.68±3.64
11	Ni/ZrO_x-400	0.2 M NaOH	71.42±2.15
12	Ni/ZrO_x-600	0.2 M NaOH	85.89±3.92
13	ZrO_x-300	0.2 M NaOH	0±0
14	ZrO_x-400	0.2 M NaOH	0±0
15	ZrO_x-500	0.2 M NaOH	0±0
16	ZrO_x-600	0.2 M NaOH	0±0

[a] Reaction conditions: AB: 3.0 mmol, H_2O: 10 mL, catalyst: 40.0 mg, temperature: 25 °C.

Table S4. Catalytic performance for AB hydrolysis over previously reported heterogeneous catalysts and this work

Entry	Catalyst	Temperature (K)	NaOH Concentration (M)	TOF (min^{-1})	E_a ($kJ\ mol^{-1}$)	Ref.
1	Ni/ZrO_x-300	298	0.2	38.68±3.64[a] 91.86±2.68[b]	38.24	This work
2	Ni/ZrO_x-400	298	0.2	71.42±2.15[a] 151.03±3.41[b]	31.97	This work
3	Ni/ZrO_x-500	298	0.2	114.41±2.58[a] 196.82±2.58[b]	21.26	This work
4	Ni/ZrO_x-600	298	0.2	85.89±3.92[a] 170.39±2.77[b]	26.80	This work
5	CoNi/α-MoC	298	0.5	321.1[b]	/	1
6	10Ni30Mo_xC/γ-Al_2O_3	298	1	75.1[a]	33.12	2
7	hcp-CuNi/C	300	1	22.64[a]	29.92	3
8	Ni/KB	298	0	7.47[a]	/	4
9	Ni/CeO_2	298	0	1.7[a]	25	5
10	Ni/CNTs	298	0	26.2[a]	32.3	6
11	NiNPs/ZIF-8	298	0.3	85.7[a]	42.70	7
12	Ni/Ti_3C_2Tx-4	298	0	161.0[a]	59.3	8
13	rGO/CoNi-N	298	0	126[a]	32.8	9
14	Ni-CeOx/Graphene	298	0	68.2[a]	28.9	10
15	Ni NPs@3D-(N)GFs	303	0	41.7[a]	/	11
16	Ni/SiO_2	303	0	13.2[a]	34.0	12

[a] the initial TOF value was calculated based on the following equation: TOF (h^{-1}) = (converted substrate (mmol))/(total metal amount (mmol))(reaction time (h)).

[b] the initial TOF value was calculated based on the following equation: TOF (h^{-1}) = (converted substrate (mmol))/(surface atoms of active metal (mmol))(reaction time (h)).

References

1 Y. Ge, X. Qin, A. Li, Y. Deng, L. Lin, M. Zhang, Q. Yu, S. Li, M. Peng, Y. Xu, X. Zhao, M. Xu, W. Zhou, S. Yao and D. Ma, *J. Am. Chem. Soc.*, 2021, 143, 628–33.

2 Y. Ren, J. Duan, X. Liu, L. Bian, Y. Fan and B. Liu, *Energ. Fuel.*, 2021, 35, 16222–16231.

3 P. Li, R. Chen, Y. Huang, W. Li, S. Zhao and S. Tian, *Appl. Catal. B: Environ.*, 2022, 300, 120725.

4 K. Guo, H. Li and Z. Yu, *ACS Appl. Mater. Interfaces*, 2018, 10, 517–525.

5 S. Akbayrak, O. Taneroğlu and S. Özkar, *New J. Chem.*, 2017, 41, 6546–6552.

6 J. Zhang, C. Chen, W. Yan, F. Duan, B. Zhang, Z. Gao and Y. Qin, *Catal. Sci. Technol.*, 2016, 6, 2112–2119.

7 P. Li, K. Aranishi and Q. Xu, *Chem. Commun.*, 2012, 48, 3173–3175.

8 B. Mo, S. Li, H. Wen, H. Zhang, H. Zhang, J. Wu, B. Li and H. Hou, *ACS Appl. Mater. Interfaces*, 2022, 14, 16320–16329.

9 P. Li, R. Chen, S. Zhao, W. Li, Y. Lin and Y. Yu, *Appl. Catal. B: Environ.*, 2021, 298, 120523.

10 Q. Yao, Z. Lu, Y. Yang, Y. Chen, X. Chen and H. Jiang, *Nano Res.*, 2018, 11, 4412–4422.

11 M. Mahyari and A. Shaabani, *J. Mater. Chem. A*, 2014, 2, 16652–16659.

12 Ö. Metin, S. Özkar and S. Sun, *Nano Res.*, 2020, 3, 676–684.